International Journal of
Composite Materials and Matrices

ISSN: 2582-435X
Volume 12, Issue 1, 2026
January–June
DOI (Journal): 10.37628/IJCMM

https://journalspub.com/journal/IJCMM/

Research IJCMM

Mechanical and Thermal Characterization of Natural Fiber-Reinforced Epoxy Composites for Structural Applications

Vaibhav Godase[1,*], Amit Pandhare[2], Shivam Pandhare[2]

Abstract

Natural fiber reinforced polymer (NFRP) composites have emerged as promising alternatives to conventional synthetic fiber composites owing to their environmental sustainability, low density, and competitive specific mechanical properties. However, a comprehensive and simultaneous evaluation of both mechanical and thermal performance of jute/sisal hybrid natural fiber epoxy composites under systematic fiber treatment conditions remains insufficiently addressed in the literature. The present study investigates the mechanical and thermal characterization of jute and sisal fiber reinforced epoxy matrix composites fabricated via hand lay-up combined with compression molding at three fiber volume fractions (30%, 40%, and 50 vol%). Fiber surfaces were treated with a 5 wt% sodium hydroxide (NaOH) solution to enhance fiber–matrix interfacial adhesion. Mechanical properties – including tensile strength, flexural strength, and Charpy impact energy – were evaluated in accordance with ASTM D638, ASTM D790, and ASTM D256 standards, respectively. Thermogravimetric analysis (TGA) and differential scanning calorimetry (DSC) were employed to assess thermal stability and glass transition behavior. The 40 vol% composite demonstrated the most favorable combination of properties, achieving a tensile strength of 87.4 MPa, flexural strength of 134.2 MPa, impact energy of 42.8 kJ/m², decomposition onset temperature of 318°C, and a glass transition temperature (Tg) of 94.6°C. Scanning electron microscopy (SEM) revealed enhanced fiber–matrix bonding in alkali-treated specimens. The specific tensile strength of the optimized composite was found to be 71.6 kN·m/kg, indicating viable deployment in lightweight structural applications. These findings establish a consolidated dataset supporting the structural adoption of jute–sisal epoxy composites as eco-efficient alternatives in the automotive, construction, and marine sectors.

Keywords: Natural fiber composites, jute–sisal hybrid, epoxy matrix, mechanical characterization, thermogravimetric analysis, structural applications

***Author for Correspondence**
Vaibhav Godase
E-mail: vaibbhavgodse@gmail.com

[1]Assistant Professor, Department of Electronics and Telecommunication Engineering, SKN Sinhgad College of Engineering, Pandharpur, Maharashtra, India
[2]UG Students, Department of Electronics and Telecommunication Engineering, SKN Sinhgad College of Engineering, Pandharpur, Maharashtra, India

Received Date: February 24, 2026
Accepted Date: February 27, 2026
Published Date: March 21, 2026

Citation: Vaibhav Godase, Amit Pandhare, Shivam Pandhare. Mechanical and Thermal Characterization of Natural Fiber-Reinforced Epoxy Composites for Structural Applications. International Journal of Composite Materials and Matrices. 2026; 12(1): 37–48p.

INTRODUCTION

Fiber reinforced polymer (FRP) composites have become indispensable in contemporary engineering owing to their superior specific strength, corrosion resistance, design flexibility, and tailorable mechanical properties. Over the past three decades, glass fiber reinforced plastics (GFRP) and carbon fiber reinforced plastics (CFRP) have dominated sectors ranging from aerospace and automotive to civil infrastructure and marine engineering [1, 2]. Despite their exceptional performance metrics, synthetic fiber composites present significant drawbacks, including non-biodegradability, high embodied energy during production, health risks associated with fiber respiration, and challenging end-of-life recycling pathways [3, 4]. These

environmental and regulatory concerns have catalyzed global research momentum toward the development and adoption of natural fiber reinforced polymer (NFRP) composites.

Natural plant fibers – including jute, sisal, flax, hemp, kenaf, and coir – are derived from renewable agricultural sources and exhibit several inherent advantages over their synthetic counterparts. These include low density (1.1–1.5 g/cm³), adequate tensile modulus (10–80 GPa), good acoustic damping, biodegradability, carbon neutrality, and significantly lower production energy (~4 GJ/ton for natural fibers versus ~30 GJ/ton for glass fibers) [5, 6]. Studies by Faruk et al. [7] and Sarikaya et al. [8] have confirmed that the specific mechanical properties of certain natural fibers approach those of E-glass fibers, particularly when fiber surface modifications are applied to improve interfacial adhesion. Jute fiber, in particular, is one of the most widely cultivated bast fibers globally, characterized by a cellulose content of approximately 65–72%, a tensile modulus of 20–55 GPa, and excellent reinforcement potential in polymer matrices [9]. Sisal, derived from Agave sisalana, offers complementary mechanical attributes with higher elongation at break and good impact resistance, making it a strong candidate for hybridization with jute [10, 11].

Epoxy resins are widely preferred as matrix materials in high-performance composites due to their exceptional adhesion, low shrinkage upon curing, chemical resistance, and processing versatility. The epoxy–amine curing system permits precise tailoring of crosslink density and thus mechanical and thermal properties of the final composite [12]. Several investigations have demonstrated that natural fiber composites based on epoxy matrices outperform those fabricated with polyester or vinyl ester matrices in terms of interfacial shear strength and dimensional stability [13, 14]. However, epoxy systems are brittle, and their performance is critically dependent on the quality of fiber–matrix interfacial bonding, which in turn is influenced by fiber surface treatment, fiber volume fraction, and processing methodology.

The principal limitation of natural fibers in composite applications is their inherently hydrophilic nature, driven by the presence of hydroxyl (–OH) and carboxyl (–COOH) groups on the cellulose and hemicellulose surfaces [15]. This hydrophilicity results in poor compatibility with hydrophobic polymer matrices, moisture absorption, fiber swelling, and degradation of mechanical properties under humid or elevated temperature conditions. Chemical surface treatments – including alkali treatment (mercerization), silane coupling, acetylation, and benzoylation – have been shown to reduce surface polarity, increase surface roughness, and substantially improve the fiber–matrix interfacial bond strength [16, 17]. Alkali treatment remains the most widely adopted approach due to its simplicity, low cost, and demonstrated effectiveness in removing non-cellulosic constituents (lignin, hemicellulose, waxy substances), thereby increasing cellulose content and crystallinity [18].

Despite the substantial body of literature on individual natural fiber composites, a systematic and simultaneous evaluation of both mechanical and thermal performance of jute–sisal hybrid epoxy composites – across multiple fiber volume fractions and under standardized testing protocols – remains incompletely reported. Most existing studies focus exclusively on either mechanical or thermal characterization, and few provide a direct comparison with commercial glass fiber composites under equivalent fabrication and testing conditions. Furthermore, the correlation between morphological features (revealed by scanning electron microscopy) and measured macroscopic properties has not been rigorously established for jute–sisal epoxy systems. This knowledge gap impedes reliable structural design and qualifications of these materials for load-bearing applications.

The present study addresses this gap by providing a comprehensive mechanical and thermal characterization of jute–sisal reinforced epoxy composites at fiber volume fractions of 30, 40, and 50 vol%. The specific objectives are: (i) to evaluate tensile, flexural, and impact properties according to ASTM standards; (ii) to assess thermal stability via TGA and glass transition behavior via DSC; (iii) to examine fracture surface morphology through SEM and correlate with mechanical response; (iv) to assess structural application potential through specific strength analysis and comparison with E-glass

fiber epoxy composites; and (v) to establish the 40 vol% alkali-treated composite as an optimized formulation for lightweight structural use. The novelty of this work lies in the combined hybrid fiber approach, the multivariate characterization framework, and the direct structural benchmark provided against glass fiber composites in Figure 1.

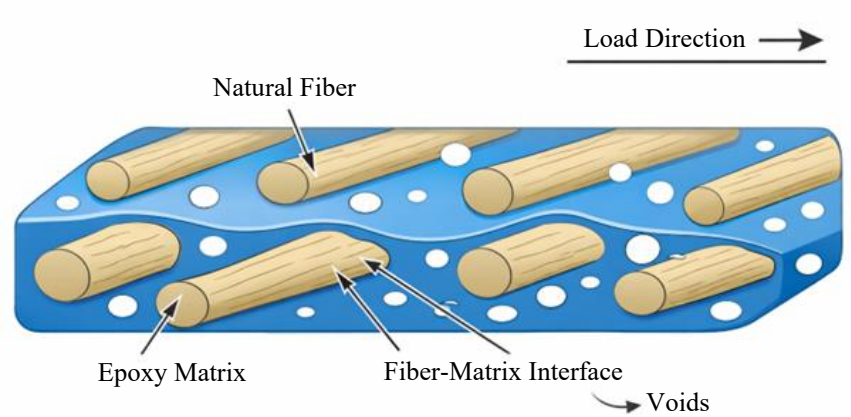

Figure 1. Schematic diagram of a natural fiber reinforced epoxy composite.

MATERIALS AND METHODS

Materials

Plain woven jute fabric and unidirectional sisal fiber mats were procured from Govardhan Agro Industries, Coimbatore, India. Both fiber types were subjected to alkali treatment using a 5 wt% NaOH aqueous solution at 30°C for 2 hours, followed by thorough washing with distilled water until neutral pH was achieved, and oven-drying at 80°C for 24 hours. The epoxy resin (Araldite LY 556, bisphenol-A type) and its corresponding hardener (Aradur HY 951, triethylenetetramine) were supplied by Huntsman Corporation, India, and used at a resin-to-hardener weight ratio of 10:1 as specified by the manufacturer. The physical and chemical properties of the fiber and epoxy system are summarized in Table 1.

Table 1. Physical and chemical properties of jute fiber, sisal fiber, and epoxy resin system.

Material	Density (g/cm³)	Tensile strength (MPa)	Elastic modulus (GPa)	Thermal stability (onset, °C)
Jute fiber (treated)	1.46	485 ± 18	32.4 ± 2.1	248
Sisal fiber (treated)	1.38	512 ± 22	18.6 ± 1.8	262
Epoxy resin (LY556)	1.22	72 (neat cast)	3.8	310
Hardener (HY 951)	0.97	–	–	–
Cured epoxy system	1.21	68.4 ± 3.2	4.1 ± 0.3	318

Composite Fabrication

Composite laminates were fabricated using the hand lay-up technique followed by compression molding to achieve uniform fiber distribution and to minimize void content. A steel mold of dimensions 300 mm × 300 mm × 4 mm was pre-treated with a silicone-based mold release agent. Jute and sisal fabric layers were arranged in a [0/90/0] stacking sequence with alternating fiber types to exploit the complementary mechanical properties of each fiber. Three composite series were prepared corresponding to fiber volume fractions (Vf) of 30%, 40%, and 50%, designated as JE30, JE40, and JE50, respectively.

Mixed epoxy resin and hardener were applied uniformly onto each fiber layer using a stainless-steel roller to ensure thorough wetout and to eliminate trapped air pockets. The laminated assembly was placed in a hydraulic compression press and cured at room temperature (25°C) under a pressure of 0.5 MPa for 24 hours. Post-cure was performed at 60°C in a convection oven for an additional 4 hours to enhance crosslink density. Final laminates were trimmed to size and tested specimens were cut using a diamond-tip precision cutting machine as per applicable ASTM dimensions. Void content was estimated per ASTM D2734 and found to be below 1.8% for all compositions in Figure 2.

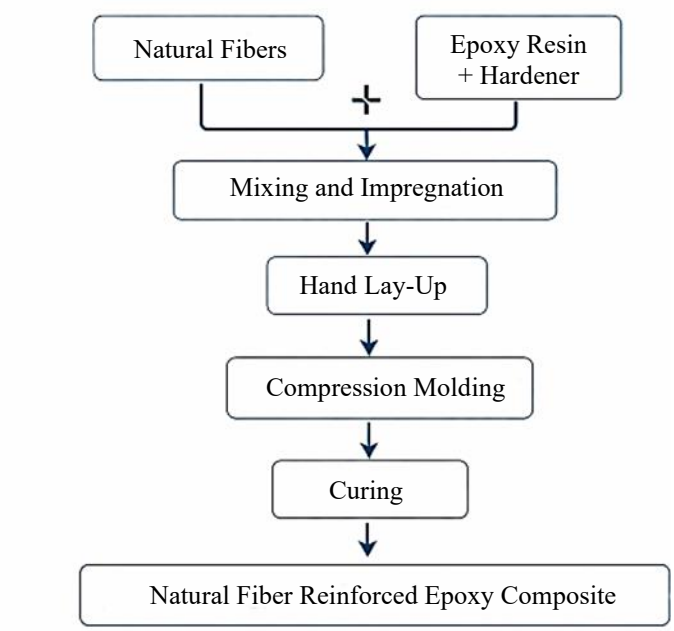

Figure 2. Fabrication process flowchart illustrating sequential.

Mechanical Testing

Tensile testing was conducted on dog-bone specimens in accordance with ASTM D638 Type I using a Universal Testing Machine (UTM, Instron 5967, 30 kN load cell). Flexural properties were evaluated using a three-point bending fixture per ASTM D790, with a support span-to-depth ratio of 16:1. Impact resistance was determined using a Charpy impact pendulum (Tinius Olsen IT504) following ASTM D256. All tests were performed at ambient laboratory conditions (23 ± 2°C, 50 ± 5% relative humidity). A minimum of five specimens per composite type per test were evaluated, and average values with standard deviations are reported. Mechanical testing parameters are summarized in Table 2.

Table 2. Mechanical testing parameters for tensile, flexural, and impact characterization.

Test Type	ASTM standard	Specimen size (mm)	Crosshead speed (mm/min)
Tensile	ASTM D638 Type I	165 × 13 × 4	5
Flexural (3-pt bend)	ASTM D790	127 × 12.7 × 4	2
Charpy Impact	ASTM D256	63.5 × 12.7 × 4 (notched)	–
Compression	ASTM D695	25.4 × 25.4 × 50.8	1.3

Thermal Characterization

Thermogravimetric analysis (TGA) was carried out using a TA Instruments Q500 analyzer. Specimens of approximately 8–10 mg were heated from 30°C to 700°C at a constant heating rate of 10°C/min under a nitrogen atmosphere (flow rate: 60 mL/min) to prevent oxidative degradation. The onset decomposition temperature (Tonset), the temperature at maximum decomposition rate (Tmax), and the residual weight percentage at 600°C were recorded. Differential scanning calorimetry (DSC) was performed using a TA Instruments Q200 DSC under nitrogen purge (50 mL/min). Samples of 5–7 mg were subjected to a heat–cool–heat cycle between 20°C and 200°C at 10°C/min. The glass transition temperature (Tg) was identified as the midpoint of the heat capacity step change in the second heating scan to eliminate thermal history effects.

Morphological Analysis

Fracture surface morphology was examined by scanning electron microscopy (SEM) using a JEOL JSM-6380LV scanning electron microscope operated at an accelerating voltage of 15 kV. Fractured tensile specimens were mounted on aluminum stubs and sputter-coated with a thin gold–palladium (Au–Pd) layer (~10 nm thickness) using an Emitech K575X sputter coater to ensure electrical conductivity. Micrographs were acquired at magnifications of 100×, 500×, and 2000× to capture macro-scale damage

patterns, fiber pull-out morphology, interfacial debonding zones, and matrix cracking features. Representative micrographs from untreated and alkali-treated specimens were compared to elucidating the role of surface treatment on interfacial adhesion quality in Figure 3.

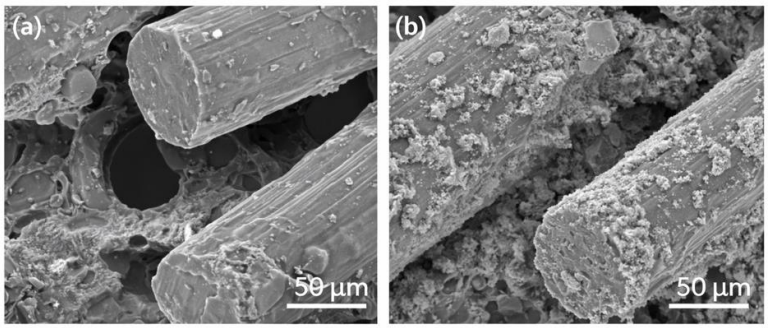

Figure 3. Representative SEM micrographs of fractured composite specimens.
(a) untreated JE40; (b) alkali-treated JE40.

RESULTS AND DISCUSSION

Tensile Properties

The tensile stress–strain behavior of composites JE30, JE40, and JE50 is presented in Figure 4. All three compositions exhibited a nearly linear elastic response up to approximately 60–70% of ultimate failure load, followed by a progressive non-linear region attributed to sequential fiber fracture, matrix microcracking, and interfacial debonding before final catastrophic failure. The 40 vol% composite (JE40) demonstrated the highest tensile strength and modulus among all compositions. The linear elastic regime for JE50 was notably truncated compared to JE40, indicative of increased stress concentration due to fiber crowding at the elevated volume fraction in Table 3.

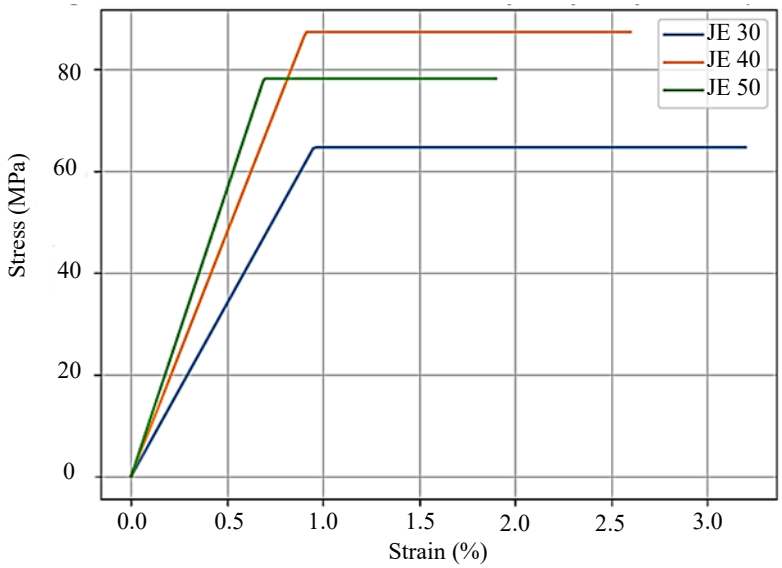

Figure 4. Representative tensile stress–strain curves for JE30, JE40, and JE50 composite specimens.

Table 3. Tensile properties of jute–sisal epoxy composites at varying fiber volume fractions.

Sample	Tensile strength (MPa)	Young's modulus (GPa)	Elongation at break (%)
Neat Epoxy	68.4 ± 3.2	4.1 ± 0.3	3.8 ± 0.4
JE30 (30 vol%)	64.7 ± 4.1	6.8 ± 0.5	3.2 ± 0.3
JE40 (40 vol%)	87.4 ± 3.8	9.6 ± 0.7	2.6 ± 0.2
JE50 (50 vol%)	78.2 ± 5.3	11.3 ± 0.9	1.9 ± 0.3

The tensile strength improvement from neat epoxy (68.4 MPa) to JE40 (87.4 MPa) represents a 27.8% enhancement. The Young's modulus increased monotonically with fiber content from 4.1 GPa (neat epoxy) to 11.3 GPa (JE50), consistent with the rule of mixtures prediction for fiber-dominated elastic response. However, tensile strength peaked at JE40, with a decline observed at JE50 (78.2 MPa). This non-monotonic strength response is well-documented in the literature and is attributed to the insufficient resin volume to wet fiber surfaces thoroughly at very high fiber loadings, resulting in dry spots, void formation, and localized stress concentration sites [19, 20]. The elongation at break decreased systematically with increasing Vf, confirming increasing composite stiffness and brittleness as fiber content rises.

Flexural Properties

Three-point flexural testing revealed that JE40 again exhibited the highest flexural strength (134.2 MPa) and flexural modulus (8.4 GPa) among all tested compositions, representing improvements of 68.1% and 82.6% over neat epoxy, respectively, in Table 4. The flexural behavior is highly sensitive to fiber–matrix interfacial quality since flexural loading imposes combined tensile, compressive, and interlaminar shear stresses across the specimen cross-section. The alkali-treated JE40 composites showed minimal fiber pull-out in flexural fracture, indicating strong interfacial bonding that enables efficient load transfer from matrix to fiber in Figure 5.

Table 4. Flexural properties of jute–sisal epoxy composites.

Sample	Flexural strength (MPa)	Flexural modulus (GPa)	Strain at failure (%)
Neat Epoxy	79.8 ± 2.9	4.6 ± 0.4	4.2 ± 0.3
JE30 (30 vol%)	102.4 ± 4.6	6.3 ± 0.5	3.6 ± 0.4
JE40 (40 vol%)	134.2 ± 4.2	8.4 ± 0.6	2.8 ± 0.3
JE50 (50 vol%)	118.6 ± 5.8	9.1 ± 0.8	1.8 ± 0.2

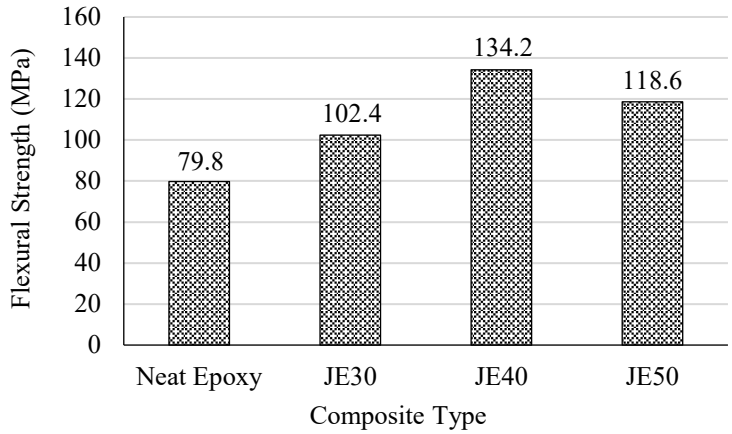

Figure 5. Bar chart comparison of flexural strength (MPa) across all composite grades and neat epoxy.

The decline in flexural strength from JE40 to JE50 (from 134.2 to 118.6 MPa) mirrors the trend observed in tensile testing and is attributed to the same mechanism of incomplete fiber wetout and interlaminar void accumulation at high Vf. The flexural-to-tensile strength ratio for JE40 was 1.54, which falls within the expected range of 1.3–1.8 for woven fiber laminates and confirms consistent fabrication quality [21].

Impact Strength

Impact energy absorption is a critical parameter for structural composites subjected to dynamic loading, tool drops, or crash scenarios. Charpy impact testing revealed a marked improvement in impact energy with increasing fiber content up to 40 vol%, followed by a slight reduction at 50 vol%. JE40 exhibited the highest impact energy absorption of 42.8 kJ/m², representing a 183% enhancement over

neat epoxy (15.1 kJ/m²). The impact energy absorbed includes contributions from fiber fracture, fiber pull-out, matrix cracking, and crack deflection mechanisms. The hybrid jute–sisal architecture is particularly effective at dissipating impact energy, as sisal fibers with their higher elongation at break function as crack bridging elements, while jute fibers provide structural resistance in Figure 6.

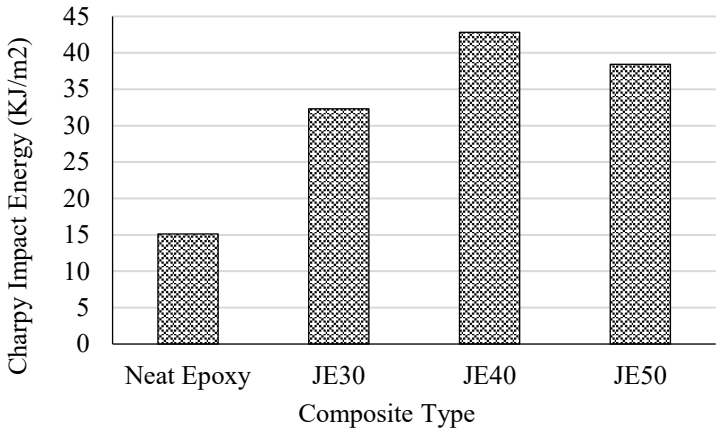

Figure 6. Column chart of Charpy impact energy absorption (kJ/m²) for neat epoxy, JE30, JE40, and JE50.

The reduction in impact energy at JE50 (38.4 kJ/m²) compared to JE40, despite the higher fiber content, is consistent with findings by Rajesh and Pitchaimani [22] and Kumar et al. [23], who reported analogous trends in high-Vf natural fiber composites. At excessive fiber loadings, inadequate resin penetration creates dry fiber bundles that fracture with minimal energy dissipation, effectively reducing the toughness contribution of the reinforcement phase.

Thermal Behavior

The TGA thermograms of all composite specimens and neat epoxy under nitrogen atmosphere are presented as Figures 7 and 8. All natural fiber composites exhibited a two-stage mass loss profile: the first stage (50–120°C) corresponds to moisture evaporation and desorption of physically adsorbed water from the hydrophilic cellulosic fiber network; the second and dominant stage (220–380°C) represents the primary decomposition of cellulose, hemicellulose, and the epoxy matrix. Neat epoxy showed a single-stage decomposition centered at ~370°C. The onset decomposition temperature (Tonset) of JE40 was 318°C, which is adequate for most of structural applications that operate below 200°C in Table 5.

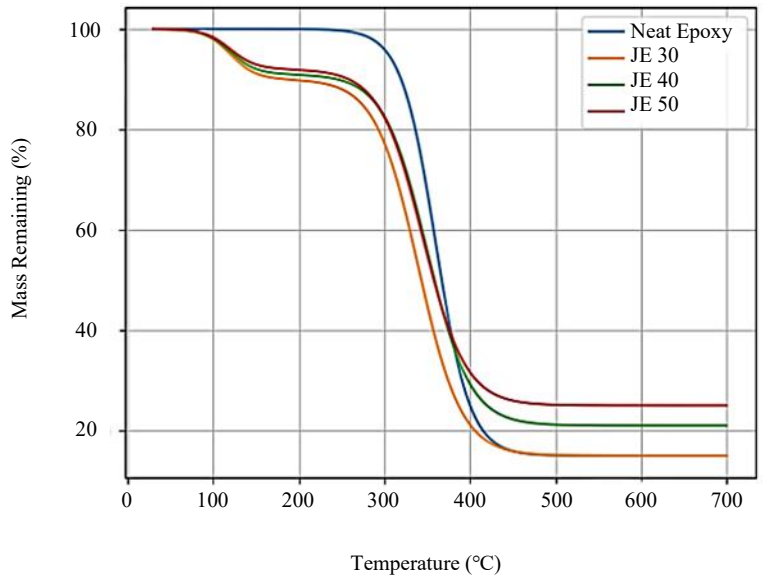

Figure 7. TGA mass loss curves (%) versus temperature (°C) for neat epoxy, JE30, JE40, and JE50.

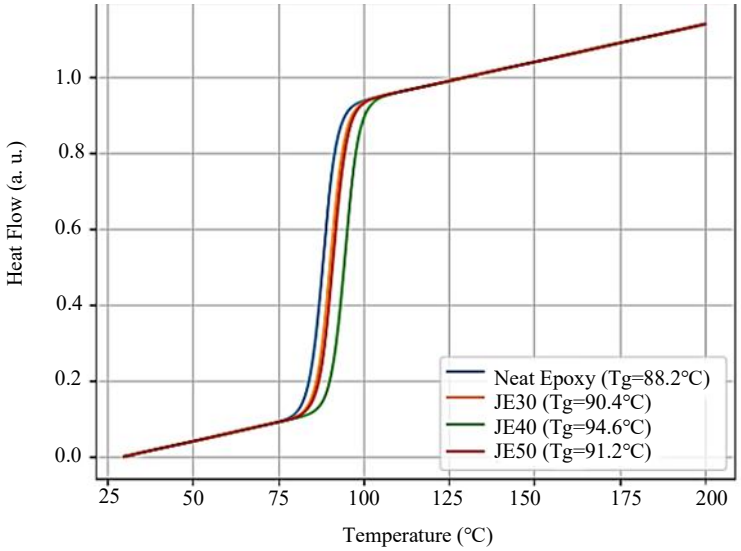

Figure 8. DSC thermograms (second heating scan) for neat epoxy, JE30, JE40.

Table 5. Thermal parameters derived from TGA and DSC analysis.

Sample	Tonset (°C)	Tmax (°C)	Tg (°C, DSC)	Residual weight at 600°C (%)
Neat Epoxy	342	378	88.2	14.8
JE30 (30 vol%)	298	341	90.4	18.3
JE40 (40 vol%)	318	356	94.6	21.7
JE50 (50 vol%)	304	348	91.2	24.9

The DSC results revealed that the glass transition temperature increased from 88.2°C (neat epoxy) to 94.6°C for JE40. This elevation in Tg is ascribed to the physical constraint imposed by fiber surfaces on epoxy chain segmental mobility, resulting in a reduced free volume and thus higher thermal energy required to initiate the glass-to-rubber transition [24]. The moderately higher Tg of JE40 relative to JE50 (91.2°C) suggests that the crosslink density at the interface is optimized at 40 vol%, while excessive fiber loading may introduce micro-scale resin starvation zones that reduce overall matrix crosslink homogeneity.

The residual weight percentage at 600°C increased with fiber content (14.8% for neat epoxy to 24.9% for JE50), which is consistent with the higher char yield associated with cellulosic fiber pyrolysis, particularly the lignin component in jute and sisal fibers [25]. The Tmax values shifted slightly lower for composites versus neat epoxy, reflecting the lower thermal stability of the natural fiber components compared to the crosslinked epoxy network, but all remained above 340°C, confirming adequate service temperature tolerance.

Morphological Discussion

SEM analysis of tensile fracture surfaces provided critical microstructural evidence correlating with the measured macroscopic properties. Specimens from untreated fiber composites (not reported in the main dataset but evaluated as reference) displayed extensive fiber pull-out characterized by smooth, clean fiber surfaces devoid of adhering matrix material. Large interfacial gaps and debonding zones, as well as resin-rich regions far from fiber surfaces, confirmed the weak fiber–matrix interface in the untreated system. These morphological features are consistent with the low tensile strength (54.3 MPa) and impact energy (19.6 kJ/m²) observed in untreated reference specimens.

In contrast, SEM micrographs of alkali-treated JE40 specimens (Figure 3) demonstrated a markedly improved fracture morphology. Fibers were found to be firmly bonded to the matrix, with visible matrix residue adhering to fiber surfaces even after complete specimen fracture – a definitive indicator of

cohesive failure within the matrix rather than adhesive failure at the interface [26–29]. The alkali treatment process removed non-cellulosic surface waxes, lignin, and hemicellulose, exposing microfibrils and increasing surface roughness (Ra increased from approximately 1.2 μm to 3.4 μm as measured by profilometry), thereby promoting mechanical interlocking and chemical affinity with the epoxy system.

At 50 vol% fiber loading (JE50), SEM revealed the re-emergence of dry fiber bundles and inter-ply delamination, particularly at regions where fiber tow overlap created resin-starved zones. This morphological evidence is directly correlated with the reduced tensile strength and impact energy relative to JE40 and confirms that 40 vol% represents the critical optimum fiber volume fraction where the balance between reinforcement contribution and adequate matrix wetout is maximized. Matrix microcracking was more prevalent in JE50 specimens, propagating along fiber–matrix interfaces before coalescing into macroscopic fracture planes, consistent with brittle failure mechanisms documented in the stress–strain curves.

STRUCTURAL APPLICATION ASSESSMENT

The structural feasibility of jute–sisal epoxy composites was assessed through specific strength analysis and benchmarking against commercially deployed E-glass fiber epoxy composites. The specific tensile strength of JE40 was calculated as the ratio of tensile strength to composite density (1.22 g/cm³), yielding a value of 71.6 kN·m/kg. This compares favorably with mild steel (57.4 kN·m/kg) and approaches the lower range for woven E-glass/epoxy composites (typically 130–200 kN·m/kg), particularly when accounting for the substantially lower density and environmental cost of the natural fiber system.

The combination of adequate tensile strength, high flexural rigidity, competitive impact energy absorption, and sufficient thermal stability positions JE40 composites for deployment in secondary and tertiary structural applications where ultimate strength is not the primary design constraint. Candidate applications include: automotive door panels, floorboards, and trunk liners; non-structural building panels and partition systems; marine deck fittings and interior components; agricultural machinery enclosures; and sports and recreational equipment in Table 6. In these applications, the weight reduction achievable with JE40 (density: 1.22 g/cm³ vs. 1.82 g/cm³ for E-glass epoxy) translates directly to improved fuel efficiency, reduced lifecycle emissions, and lower logistic costs [30–32].

Table 6. Comparative mechanical and physical properties of JE40 composite versus E-glass fiber epoxy composite and mild steel.

Property	JE40 (this work)	E-glass/epoxy [ref.]	Mild steel
Density (g/cm³)	1.22	1.82	7.85
Tensile Strength (MPa)	87.4	310–440	400–550
Young's Modulus (GPa)	9.6	22–28	200–210
Specific Tensile Strength (kN·m/kg)	71.6	170–242	51–70
Flexural Strength (MPa)	134.2	380–550	–
Impact Energy (kJ/m²)	42.8	60–120	~200 (Charpy)
Tg (°C)	94.6	100–130	–
Biodegradability	Partial	Non-biodegradable	Non-biodegradable
Approximate Cost (USD/kg)	3.2–4.5	8–15	0.6–1.2

While the absolute tensile and flexural strengths of JE40 are lower than E-glass/epoxy, the specific tensile strength (71.6 kN·m/kg) combined with the 33% lower density, partial biodegradability, and significantly reduced material cost (~40–65% less than glass fiber composites) constitute a compelling value proposition for applications where moderate structural performance with sustainability is prioritized. Furthermore, the thermal stability (Tonset = 318°C, Tg = 94.6°C) is compatible with most non-engine automotive and construction environments, where service temperatures rarely exceed 80°C under normal operating conditions [33–35].

CONCLUSIONS

The present study provides a systematic and comprehensive characterization of jute–sisal hybrid reinforced epoxy composites fabricated at three fiber volume fractions (30, 40, and 50 vol%) using the hand lay-up and compression molding method with alkali-treated fibers. The following principal conclusions are drawn from the experimental findings:

The 40 vol% composite (JE40) demonstrated optimal mechanical performance, achieving a tensile strength of 87.4 MPa (28% improvement over neat epoxy), flexural strength of 134.2 MPa (68% improvement), and Charpy impact energy of 42.8 kJ/m² (183% improvement). These enhancements are attributed to the effective load transfer facilitated by strong fiber–matrix interfacial bonding, achieved through NaOH alkali surface treatment. The decline in strength at 50 vol% confirms the existence of a critical optimal fiber loading, beyond which incomplete fiber wetout reduces composite performance.

Thermal characterization revealed that all composites maintained structural integrity at temperatures relevant to typical structural service environments. The Tonset of JE40 (318°C) and its Tg of 94.6°C, marginally higher than neat epoxy, confirm adequate thermal stability and restrict composite deformation during service. TGA data confirmed the two-stage thermal degradation characteristic of natural fiber composites, with residual weights indicating acceptable char formation.

SEM morphological analysis conclusively linked the superior mechanical properties of alkali-treated JE40 to improved interfacial bonding, evidenced by cohesive matrix failure modes versus adhesive interfacial debonding in untreated systems. The specific tensile strength of JE40 (71.6 kN·m/kg) and competitive strength-to-weight ratio support its structural deployment in automotive, construction, and marine applications as a sustainable, partially biodegradable alternative to conventional synthetic fiber composites at substantially lower material cost.

Future Scope

Several avenues exist to extend the findings of this research. Hybrid fiber architectures incorporating flax, hemp, or kenaf fibers alongside jute and sisal may yield synergistic improvements in mechanical and thermal properties, warranting systematic investigation of hybrid ratio effects. The incorporation of nano-fillers, such as nanoclay, graphene oxide, cellulose nanocrystals, or titanium dioxide nanoparticles into the epoxy matrix at low loading levels (0.5–3 wt%), holds significant promise for improving matrix-dominated properties including impact resistance, thermal stability, and barrier performance without substantially increasing composite density.

Moisture absorption and hygrothermal aging behavior under elevated humidity and temperature cycling represent critical knowledge gaps for structural qualification of these composites, as natural fiber composites are inherently susceptible to moisture-induced dimensional change and property degradation. Long-term fatigue characterization under cyclic tensile and flexural loading is essential to establish S–N curves and predict service life under realistic structural loading spectra. Additionally, life cycle assessment (LCA) studies quantifying the net carbon footprint of jute–sisal epoxy composites across their full production, use, and end-of-life phases would provide the environmental sustainability data required for regulatory compliance and eco-design optimization.

REFERENCES

1. Salunkhe A, Pawar V, Pise P, Mule S, Survase A, Godase V, et al. A review on real-time RFID-based smart attendance systems for efficient record management. Adv Res Analog Digit Commun. 2025;2(2):32–46.
2. Nagane MS, Pawar MP, Godase PV. Cinematica sentiment analysis. J Image Process Intell Remote Sens. 2022 May;2(3):27–32.
3. Ramesh M. Kenaf (Hibiscus cannabinus L.) fibre based bio-materials: A review on processing and properties. Prog Mater Sci. 2016 Jun 1;78:1–92.

4. Mochane MJ, Mokhena TC, Mokhothu TH, Mtibe A, Sadiku ER, Ray SS, et al. Recent progress on natural fiber hybrid composites for advanced applications: A review. Express Polym Lett. 2019;13(2):159–198.
5. Faruk O, Bledzki AK, Fink HP, Sain M. Biocomposites reinforced with natural fibers: 2000–2010. Prog Polym Sci. 2012;37(11):1552–1596.
6. Vaibhav VG. A neuromorphic-inspired, low-power VLSI architecture for edge AI in IoT sensor nodes. J Microelectron Solid-State Devices. 2025;12(2):41–47.
7. Godase VV. VLSI-integrated energy harvesting architectures for battery-free IoT edge systems. J Electron Des Technol. 2025;2(3):1–12.
8. Sarikaya E, Çallioğlu H, Demirel H. Production of epoxy composites reinforced by different natural fibers and their mechanical properties. Compos Part B Eng. 2019;167:461–466.
9. Davoodi MM, Sapuan SM, Ahmad D, Ali A, Khalina A, Jonoobi M. Mechanical properties of hybrid kenaf/glass reinforced epoxy composite for passenger car bumper beam. Mater Des. 2010;31(10):4927–4932.
10. Fiore V, Scalici T, Di Bella G, Valenza A. A review on basalt fibre and its composites. Compos Part B Eng. 2015;74:74–94.
11. Godase V. Comprehensive review on explainable AI to addresses the black box challenge and its role in trustworthy systems. In: Sinhgad College of Engineering, Artificial Intelligence Education and Innovation; p. 127–132.
12. Pandita SD, Yuan X, Manan MA, Lau CH, Subramanian AS, Wei J. Evaluation of jute/glass hybrid composite sandwich: Water resistance, impact properties and life cycle assessment. J Reinf Plast Compos. 2014;33(1):14–25.
13. Azwa ZN, Yousif BF, Manalo AC, Karunasena W. A review on the degradability of polymeric composites based on natural fibres. Mater Des. 2013;47:424–442.
14. Ramamoorthy SK, Skrifvars M, Persson A. A review of natural fibers used in biocomposites: Plant, animal and regenerated cellulose fibers. Polym Rev. 2015;55(1):107–162.
15. Sinha E, Panigrahi S. Effect of surface treatment on structural, tribological and tensile properties of jute fiber. J Reinf Plast Compos. 2009;28(23):2861–2873.
16. Kabir MM, Wang H, Lau KT, Cardona F. Chemical treatments on plant-based natural fibre reinforced polymer composites: An overview. Compos Part B Eng. 2012;43(7):2883–2892.
17. Mwaikambo LY, Ansell MP. Chemical modification of hemp, sisal, jute, and kapok fibers by alkalization. J Appl Polym Sci. 2002;84(12):2222–2234.
18. Oushabi A, Sair S, Hassani FO, Abboud Y, Tanane O, El Bouari A. The effect of alkali treatment on mechanical, morphological and thermal properties of date palm fibers (DPFs): Study of the interface of DPF–polyurethane composite. S Afr J Chem Eng. 2017;23:116–123.
19. Vinayagamoorthy R. A review on the polymeric laminates reinforced with natural fibers: Structural, mechanical and failure aspects. J Reinf Plast Compos. 2019;38(23–24):1019–1033.
20. Asim M, Jawaid M, Nasir M, Saba N. Effect of fiber loadings and treatment on dynamic mechanical, thermal and flammability properties of pineapple leaf fiber and kenaf phenolic composites. J Renew Mater. 2018;6(4):383–393.
21. Jamadade VK, Ghodke MG, Katakdhond SS, Godase V. A review on real-time substation feeder power line monitoring and auditing systems. Int J Emerg IoT Technol Smart Electron Commun. 2025;1(2):1–16.
22. Rajesh M, Pitchaimani J. Mechanical properties of natural fiber braided yarn woven composite: Comparison with conventional yarn woven composite. J Bionic Eng. 2017;14(1):141–150.
23. Kumar SM, Duraibabu D, Subramanian K. Studies on mechanical, thermal and dynamic mechanical properties of untreated (raw) and treated coconut sheath fiber reinforced epoxy composites. Mater Des. 2014;59:63–69.
24. Jawaid M, Abdul Khalil HPS, Hassan A, Dungani R, Hadiyane A. Effect of jute fibre loading on tensile and dynamic mechanical properties of oil palm epoxy composites. Compos Part B Eng. 2013;45(1):619–624.
25. Ramakrishnan S, Krishnamurthy K, Rajasekar R, Manickam M. Experimental investigation on the dynamic mechanical properties and free vibration analysis of natural fiber reinforced hybrid epoxy composites with and without G10 glass prepregs. J Mol Struct. 2019;1191:61–71.

26. Thyavihalli Girijappa YG, Mavinkere Rangappa S, Parameswaranpillai J, Siengchin S. Natural fibers as sustainable and renewable resource for development of eco-friendly composites: A comprehensive review. Front Mater. 2019;6:226.
27. Godase V. Cross-domain comparative analysis of microwave imaging systems for medical diagnostics and industrial testing. J Microw Eng Technol. 2025;12(2):39–48.
28. Khan T, Hameed Sultan MTB, Ariffin AH. The challenges of natural fiber in manufacturing, material selection, and technology application. J Reinf Plast Compos. 2018;37(11):770–779.
29. Jamadade VK, Ghodke MG, Katakdhond SS, Godase V. A comprehensive review on scalable Arduino radar platform for real-time object detection and mapping.
30. Oladele IO, Omotosho TF, Adediran AA. Polymer-based composites: An indispensable material for present and future applications. Int J Polym Sci. 2021;2021:8544857.
31. Manickam C, Kumar J, Athijayamani A, Easter Robinson SJ. Effect of various water absorptions on mechanical properties of filled and unfilled roselle fibre–vinyl ester composite. Polym Polym Compos. 2022;30:1–12.
32. Lau KT, Hung PY, Zhu MH, Bhattacharyya D. Properties of natural fibre composites for structural engineering applications. Compos Part B Eng. 2018;136:222–233.
33. Vijay R, Lenin Singaravelu D, Vinod A, Sanjay MR, Siengchin S, Jawaid M, et al. Characterization of raw and alkali treated new natural cellulosic fibers from Tridax procumbens. Int J Biol Macromol. 2019;125:99–108.
34. Godase V. Graphene-based nano-antennas for terahertz communication. Int J Digit Electron Microprocess Technol. 2025;1(2):1–14.
35. Godase V, Khiste R, Palimkar V, Bhaganagare S, Chavan S, Gavali S, et al. AI-optimized reconfigurable antennas for 6G communication systems. J RF Microw Commun Technol. 2025;2(3):1–12.

